JOURNAL OF CONTENT VALIDATION 2026, VOL 2, ISSUE 1, 101-112
ISSN: 3093-8317, https://doi.org/10.53272/XXXX, www.cvsgm.org

JOURNAL OF CONTENT VALIDATION ISSN: 3093-8317

ANALYTICAL SOLUTION OF BUOYANCY FORCE EFFECTS ON MHD BOUNDARY LAYER

Wahid Minar[1*], Minhaj Kabir[2]

[1 2] *Department of Mathematics, City University, Kuala Lumpur, Malaysia*

**Corresponding Author Email: wahidminar@portal.city.edu.my*

Received: 11 December 2025 • Accepted: 22 March 2026 • Published: 19 April 2026

Abstract

The dimensionless, unstable, coupled, linear perturbation a technique is utilised to resolve equations with partial differentials in the research of buoyancy pressure results on non-Newtonian Jeffrey fluid go with the drift all through unsteady warmness and mass switch in the presence of a temperature gradient warmth supply and a primary chemical response within side the transferring species. Analyses and graphical displays are provided for all pertinent flow parameters. Graphs and tables are used to quantify and discuss the impacts of different flow quantities on temperature, concentration, frictional pressure, the rate factor, and the fee of mass and warmth transmission.

***Keywords**: Heat source, Thermal radiation, Chemical reaction and Jeffrey fluid.*

INTRODUCTION

In the industrial sector, the rate of heat transmission has a substantial impact on production costs and product quality. One of the key technical obstacles for high-tech businesses, transformers, vehicle engines and many other technological gadgets is efficient heating and/or cooling. Common fluids' thermal conductivity, including that of water, air and motor lubricants, can be increased. in a porous fluid-saturated media, Angirasa, D. et al. [1] described linked heat and mass transport based on spontaneous convection with opposing buoyancy effects. In their investigation of the combined effects of thermal radiation, Ohmic heating, and mixed convective heat transport in a porous medium, Pal, D. et al. [2] examined the effects of buoyancy and chemical processes. The effects of buoyancy on hydromagnetic unsteady flow via a porous channel with suction/injection are evaluated computationally. was taken into consideration by Makinde, O. D. et al. in their study [3]. The effects of thermal buoyancy force on produced flow were used by Anika, N. et al. [4] while accounting for hall and ion-slip current. Chang, C. J. et al. initially reported the natural convection flows in a vertical.

Open tube created by the combined buoyancy effects of temperature and mass diffusion in [5]. Zueco, J. et al. [6] carried out computer modelling of chemically reactive buoyancy-driven heat and mass flow through a horizontal cylinder in a non-Darcian environment with significant porosity. In their study [7], Chinyoka, T. et al. investigated the impact of buoyancy on an asymmetric convective cooling reactive third-grade fluid unstable MHD flow.

While many of the fluids used in manufacturing do not deviate from Newton's law of viscosity, this includes Paints, food ingredients, detergents, polymeric liquids, molten polymers, and lubricants are just a few examples. To put it another way, these fluids' viscosities have a variety of responses to shear stress, and their shear stress and shear rate have a connection that is not straight-line (Alam et al., 2025). The resulting equations are more complicated as a result of the fluid features, and the classical Newtonian models are inadequate to describe and predict a significant portion of the important behaviour of such fluids. As a result, a number of constitutive equations can be used to characterise the behaviour of non-Newtonian fluids. Rundora, L. et al. [8] examined the effects of buoyancy on fluid flow with unpredictable reactive variables in a porous channel. Waqas, M. et al. [9] made the discovery of the Simulation of magneto hydrodynamics and radiative heat transfer in Jeffrey nanofluid's convectively heated stratified flow. positive and negative It was observed in [10] that Azad, A. K. et al. performed a numerical analysis of the characteristics of heat and mass transfer in a closed environment with variable buoyancy ratio. The effects of buoyancy on the MHD flow of a nanofluid over a stretching sheet with chemical reaction were discovered by Chanie, A. G. et al. [11]. Sharma, R. P. et al. [12] discussed the effects of buoyancy on an unsteady MHD fluid flow that was spinning and chemically interacting across a plate. Kebede, T. et al. [13] gift the warmth and mass switch research in an unsteady float of tangent hyperbolic nanofluid throughout a shifting wedge with buoyancy and dissipation effects. The Soret and Dufour mechanism on unsteady heat and mass transfer flow in the presence of viscous dissipation, thermal buoyancy, mass buoyancy and visco elasticity was explained by Falodun, B. O. et al[14]. Iqbal, Z. et al. [15] created a study of the consequences of buoyancy in an unstable Maxwell nanofluid stagnation point flow over a vertically extended sheet with Joule heating (Mohd Pauzi & Shahadat Hossen, 2025).

A time-dependent, non-Newtonian Jeffrey fluid float in the course of risky warmth and mass switch within side the presence of a warmth supply with a temperature gradient, thermal radiation, and chemical reactions through an infinite plate has not received much attention in the literature, as far as the writers are aware. For the collection of linear partial differential equations, analytical solutions based on the perturbation method are given. The effects of several dimensional less factors in graphs and tables, extensive research is done on velocity, temperature, concentration, skin-friction coefficient, Nusselt number, and Sherwood numbers (Rashed et al., 2025).

MATHEMATICAL FORMULATION

A semi-infinite plate is passed by a viscous, incompressible, electrically conducting, radiating, and chemically reactive fluid toward the vertical direction in the presence of a uniform magnetic field B_0 that is applied perpendicular to the fluid flow is examined in this chapter using an unsteady MHD model. Let's assume that the x-axis is taken on the plate and that the y-axis is normal to the plate. When $t^* \leq 0$,, the fluid and plate are both initially in a stationary state where the temperature and concentration are both constant. The velocity is zero when $t^* > 0$. The plate's temperature and concentration are both increased to T^*_w and C^*_w at the same time. Since the magnetic Reynolds number of the flow is believed to be very low, it is also assumed that the induced magnetic field is insignificant for free convection flow. The viscous dissipation in the energy equation is insignificant. According to the standard Boussinesq approximation, the effects of density variation with temperature and concentration are solely taken into account for the body force term. The fluid under consideration is grey, a non-scattering medium that absorbs and emits radiation (Rahman, Hossain, et al., 2025). The physical variables are only spatial functions coordinates y* and t* because it is assumed that the direction of the fluid flow is along the x*-axis.

The governing equations listed below are

Conservation of momentum

$$\frac{\partial u^*}{\partial t^*} = g\beta_C^*(C^* - C_\infty^*) + g\beta_T^*(T^* - T_\infty^*) - \frac{\sigma B_0^2}{\rho}u^* + v\left(\frac{1}{1+\lambda}\right)\frac{\partial^2 u^*}{\partial y^{*2}} \quad (1)$$

Conservation of energy

$$\frac{\partial T^*}{\partial t^*} = -\frac{1}{\rho C_p}\frac{\partial q_r}{\partial y^*} + Q^*\frac{\partial}{\partial y^*}(T^* - T_\infty^*) + \frac{k}{\rho C_p}\frac{\partial^2 T^*}{\partial y^{*2}} \quad (2)$$

Equation of species diffusion

$$\frac{\partial C^*}{\partial t^*} = -Kr\,(C^* - C_\infty^*) + D_m\frac{\partial^2 T^*}{\partial y^{*2}} \quad (3)$$

The initial boundary conditions are

$$\begin{aligned} &t^* \le 0,\ C^* = C_\infty^*,\quad T^* = T_\infty^*,\ u^* = 0 \quad \text{for all } y^*, \\ &t^* > 0,\ C^* = C_w^*,\quad T^* = T_w^*,\ \ u^* = 0 \quad \text{at } y^* = 0, \\ &\qquad C^* \to C_\infty^*,\ \ T^* \to T_\infty^*,\ u^* \to 0 \text{ as } y^* \to \infty. \end{aligned} \quad (4)$$

Where $u^*, \lambda, B_0, v, q_r, Q, \sigma, D_m, t, \kappa, \rho, \theta^*, \emptyset^*, C_p, C_{s,} K_T\ and K_r$ are respectively the Velocity of the fluid in the x^*- direction, Jeffrey fluid parameter, external magnetic field, kinematic viscosity, radiative heat flux, heat source, electric conductivity, Coefficient of mass diffusivity ,time, thermal conductivity, fluid density, temperature of the fluid near the plate, Species concentration, Specific heat at constant pressure, Concentration susceptibility and chemical reaction parameter.

According to the Rosseland approximation, the radiative heat flux is calculated as follows: $q_r = -\frac{4\sigma^*}{3k^*}\frac{\partial T^{*4}}{\partial y^*}$ (5)

The Taylor series enlargement of T_∞^* as is used to expand the linear temperature function T^{*^4}.

$$T^{*^4} = 4T_\infty^{*^3}T^* - 3T_\infty^{*^4}. \quad (6)$$

The equation (2) then reduces to given the results of equations (5) and (6).

$$\frac{\partial T^*}{\partial t^*} = -\frac{16\sigma^* T_\infty^{*3}}{3\rho C_p k^*}\frac{\partial^2 T^*}{\partial y^{*2}} + Q^*\frac{\partial}{\partial y^*}(T^* - T_\infty^*) + \frac{k}{\rho C_p}\frac{\partial^2 T^*}{\partial y^{*2}} \quad (7)$$

The non-dimensional quantities listed below are

$$\theta = \frac{(T^* - T_\infty^*)}{(T_w^* - T_\infty^*)}, Gm = \frac{vg\beta_C^*(C_w^* - C_\infty^*)}{u_0^3}, y = \frac{u_0}{v}y^*, t = \frac{u_0^2}{v}t^*, \phi = \frac{(C^* - C_\infty^*)}{(C_w^* - C_\infty^*)}, Gr = \frac{vg\beta_T^*(T_w^* - T_\infty^*)}{u_0^3},$$

$$M = \frac{\sigma B_0^2 v}{\rho u_0^2}, Ec = \frac{u_0^2}{C_p(T_w^* - T_\infty^*)}, \Pr = \frac{\rho v C_p}{k}, Q = \frac{Q^* v}{\rho C_p u_0^2}, R = \frac{16\sigma^* T_\infty^{*3}}{3k^* k}, a = \frac{v}{u_0^2}a^*, Sc = \frac{v}{D_m}, u = \frac{u^*}{u_0}.$$

(8)

The following non-dimensional forms are then reduced using the equations (1), (3), (4), and (7) in light of (8).

$$\frac{\partial u}{\partial t} = Gr\,\theta + Gm\,\phi + \left(\frac{1}{1+\lambda}\right)\frac{\partial^2 u}{\partial y^2} - Mu \quad (9)$$

$$\frac{\partial\theta}{\partial t}=Q\frac{\partial\theta}{\partial y}+\left(\frac{1+R}{\Pr}\right)\frac{\partial^2\theta}{\partial y^2} \quad (10)$$

$$Sc\frac{\partial\phi}{\partial t}=-Sc\,Kr\,\phi+\frac{\partial^2\phi}{\partial y^2} \quad (11)$$

The associated boundary conditions become

$$\begin{aligned} &t \le 0,\ \phi=0,\ \theta=0,\ u=0 \text{ for all } y,\\ &t>0,\ \phi=1,\ \theta=1,\ u=0 \text{ at } y=0,\\ &\qquad \phi\to 0,\ \theta\to 0,\ u\to 0 \text{ as } y\to\infty. \end{aligned} \quad (12)$$

SOLUTION OF THE PROBLEM

We observe that all incompressible fluids and it is assumed that the solutions of the forms are valid $Ec<<1$ for all incompressible fluids in order to solve the equations (9) to (11), under the boundary conditions (12),

$$\begin{aligned} u(y,t) &= u_0(y) + Ec\,e^{-nt}\,u_1(y) + O(Ec^2)\\ \theta(y,t) &= \theta_0(y) + Ec\,e^{-nt}\,\theta_1(y) + O(Ec^2)\\ \phi(y,t) &= \phi_0(y) + Ec\,e^{-nt}\,\phi_1(y) + O(Ec^2) \end{aligned} \quad (13)$$

When the equations (9) to (11) are replaced with equations (13) and the coefficient of the same degree terms are equalised, the terms bigger than $O(Ec^2)$ are ignored.

The ordinary differential equations that we obtain are provided by $\left(\frac{1}{1+\lambda}\right)u_0''-Mu_0=-Gr\,\theta_o-Gm\,\phi_o$ (14)

$$\left(\frac{1}{1+\lambda}\right)u''_1-(M-n)u_1=-Gr\,\theta_1-Gm\,\phi_1 \quad (15)$$

$$\left(\frac{1+R}{\Pr}\right)\theta_0''+Q\,\theta_0'=0 \quad (16)$$

$$\left(\frac{1+R}{\Pr}\right)\theta_1''+Q\,\theta_1'+n\,\theta_1=0 \quad (17)$$

$$\phi_0''-Kr\,Sc\,\phi_0=0 \quad (18)$$

$$\phi_1''-Sc\,(Kr-n)\,\phi_1=0 \quad (19)$$

These boundary conditions are appropriate.

$$\begin{aligned} &t\le 0,\phi_0=0,\phi_1=0,\theta_0=0,\theta_1=0,u_0=0,u_1=0 \text{ for all } y,\\ &t>0,\phi_0=1,\phi_1=0,\theta_0=1,\theta_1=0,u_0=0,u_1=0 \text{ at } y=0,\\ &\phi_0\to 0,\phi_1\to 0,\theta_0\to 0,\theta_1\to 0,u_0\to 0,u_1\to 0 \text{ as } y\to\infty. \end{aligned} \quad (20)$$

The equations' answers are

$$u(y,t)=(B_1+B_2)e^{-MA_3y}-\left(B_1e^{-A_2Qy}+B_2e^{-A_1y}\right) \quad (21)$$

$$\theta(y,t) = e^{-A_2 Q y} \tag{22}$$

$$\phi(y,t) = e^{-A_1 y} \tag{23}$$

Skin-friction coefficient

The formula for the skin-friction coefficient at y=0 is

$$\tau = -\left(\frac{1}{1+\lambda}\right)\left(\frac{\partial u}{\partial y}\right)_{y=0}$$

$$\tau = -\left(\frac{1}{1+\lambda}\right)\left[-MA_3\left(B_1 + B_2\right) + A_2 Q B_1 + A_1 B_2\right]$$

Nusselt number

Nusselt number at y = 0 is given by

$$Nu = -\left(\frac{\partial \theta}{\partial y}\right)_{y=0}$$

$$Nu = A_2 Q$$

Sherwood number

Sherwood number at y = 0 is given by

$$Sh = -\left(\frac{\partial \phi}{\partial y}\right)_{y=0}$$

$$Sh = A_1$$

where

$$A_1 = Kr\,Sc, A_2 = \frac{\Pr}{1+R}, A_3 = 1+\lambda$$

$$B_1 = \frac{Gr}{A_2^2 Q^2 - MA_3}, B_2 = \frac{Gm}{A_1^2 - MA_3}.$$

Result and Discussion:

In relation to this physical issue, graphs and tables have been used to discuss the velocity, temperature, concentration, rate of velocity, rate of heat transfer, and rate of mass transfer by giving numerical values to parameters like the magnetic parameter (M), thermal Grashof number (Gr), mass Grashof number (Gm), Jeffrey fluid parameter (λ), Schmidt number (Sc), chemical reaction parameter (Kr), heat source parameter (Q>0), Prandtl number (Pr) and thermal radiation parameter (T). Figures (1) through (8) show how the region's buoyancy-assist flow (Gr > 0, Gm > 0) and buoyancy-oppose flow (Gr < 0, Gm < 0) are currently behaving.

The effects of the magnetic parameter (M), Prandtl number (Pr), and heat source parameter (Q>0) on the fluid velocity are depicted in Figures (1) to (3), which correspond to the buoyancy-assisting and -opposing regions. It is evident from the diagram that the fluid velocity decreases in the region that promotes buoyancy while demonstrating a reversal trend in the region that opposes buoyancy. The momentum boundary layer weakens in the buoyancy-assisting zone, as shown by this graph. The Lorentz force causes velocity to decrease as the magnetic parameter rises, which lowers the velocity magnitude. Additionally, an increase in Pr causes the fluid's viscosity to improve or its thermal diffusivity to decrease, both of which result in a gradual drop in the fluid's flow velocity. The buoyancy-assisting and -opposing zones are affected by the velocity-representing parameters R and Gr, Gm, as shown in Figures (4) to (5). In the region that promotes buoyancy, the fluid velocity increases, whereas the region that opposes buoyancy shows a reversal trend. This is shown by the diagram. The buoyancy-opposing zone of this graph exhibits a weakening of the momentum boundary layer. Figures (4) to (5) illustrate the effects of parameter R and Gr, Gm. The effects of the Schmidt number (Sc), the chemical reaction parameter (Kr), and the Jeffrey fluid parameter (λ.) on the velocity profile in the buoyancy-forced regions that are both helping and opposing are shown in Figures (6) to (8). As,Sc or Kr increase, the fluid's velocity decreases while trending in the opposite direction in the buoyancy-opposing region. This graph demonstrates how the momentum boundary layer becomes weaker in the buoyancy-opposing zone for both locations (Alam et al., 2025).

Figures (9) and (10) illustrate how the temperature field changes when the Prandtl number (Pr) and the heat source parameter (Q>0) increase. The temperature curve abruptly flattens when thermal diffusivity declines with rising Pr and Q values. the ratio of thermal diffusivity to kinematic viscosity is represented by the Prandtl number (Pr), where Additionally, a heat source is indicated by the positive Q sign, whereas a heat sink is shown by the negative Q sign (heat sink). The production of heat from the surface, which increases the temperature of the flow field, is what is meant by a heat source in terms of physics. As the heat source parameter rises, temperature therefore rises exponentially and quickly from the surface. The influence of the heat source parameter on temperature distribution is strongly correlated with the heat sink parameter. From the moment of bodily emergence, these effects are plainly fostered. Figure depicts how R affected the temperature distribution (11). As the radiation parameter R increases, the fluid warms and the thermal field becomes stronger (Hossen et al., 2023).

Figures (12) and (13) show how concentration is impacted by the Schmidt number (Sc) and chemical reaction (Kr) (13). The concentration is shown to drop as Sc or Kr on the fluid flow increases. This is due to the straightforward fact that the chemical in this system is consumed during the chemical process, which results in a decrease in concentration. The most significant effect of the first order reaction is its inclination to decrease overshoot in the profiles of the matter concentration in the solute physical phenomenon.

The table displays the impacts of the Sherwood, Nusselt, and skin-friction coefficients. The Nusselt number solely decreases with rising R and increases with growing Pr or Q. The Sherwood number climbs when Sc or Kr rises. The skin-friction coefficient increases with increases in, Pr, Q, Sc, or Kr and decreases with increases in M or R when buoyancy is helping. If there is a competing region, the trend is the other way around.

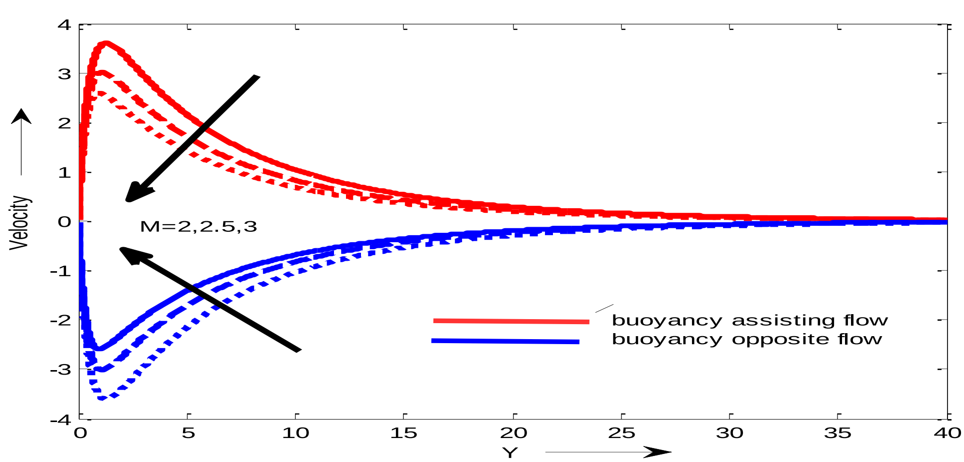

Fig.1. Consequence of *M* on Velocity

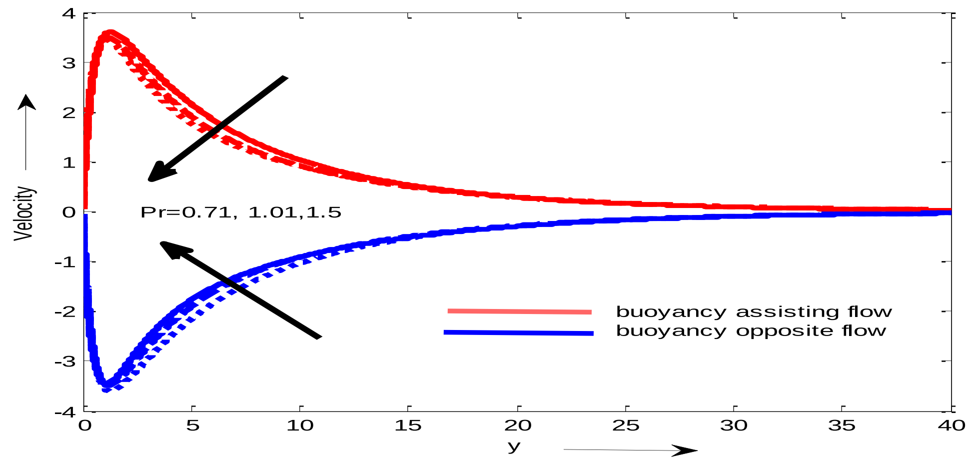

Fig.2. Consequence of *Pr* on Velocity

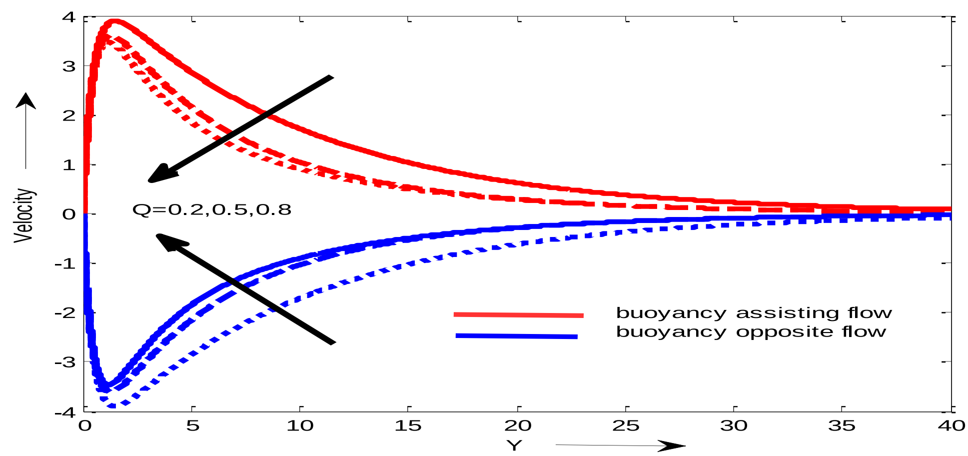

Fig.3. Consequence of *Q* on Velocity

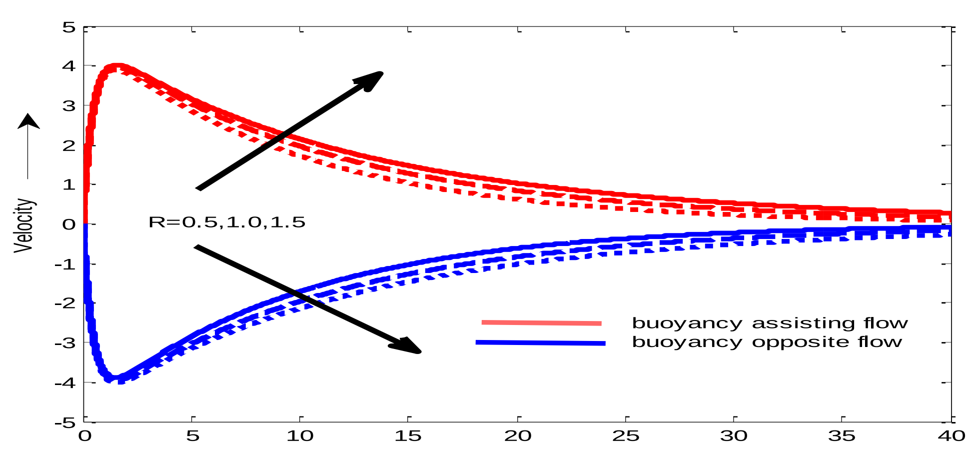

Fig.4.Consequence of *R* on Velocity

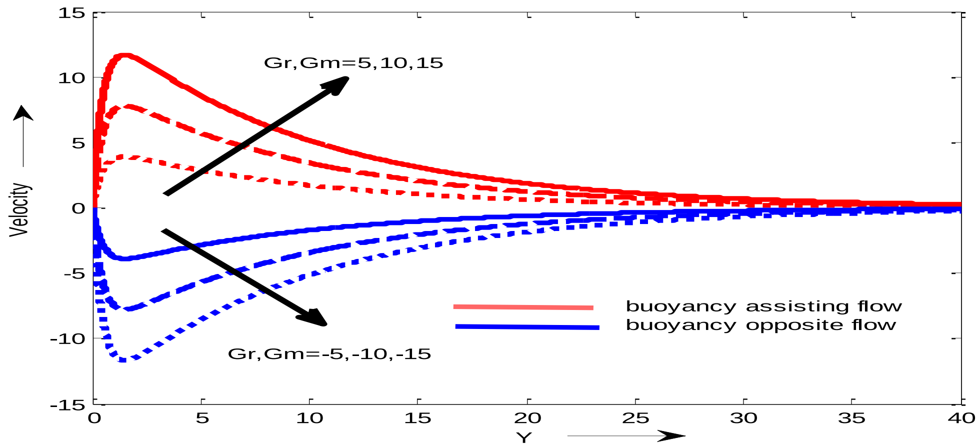

Fig.5.Consequence of *Gr, Gm* on Velocity

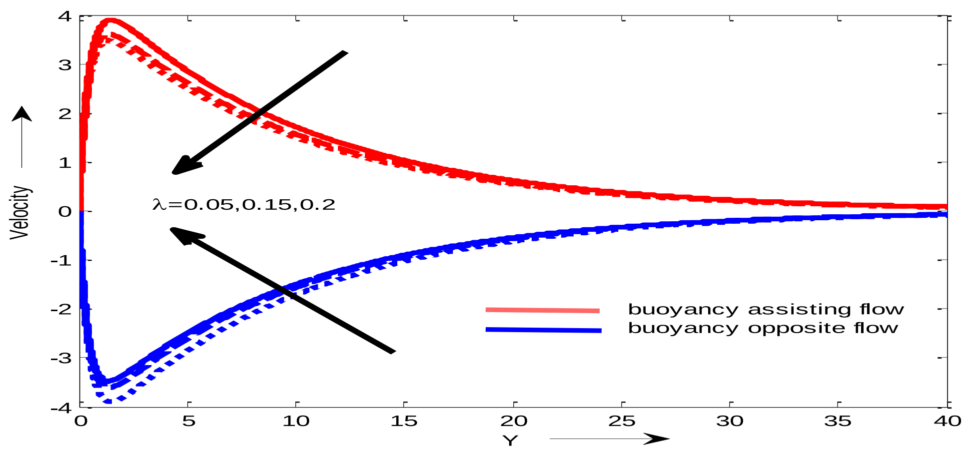

Fig.6. Consequence of *λ* on Velocity

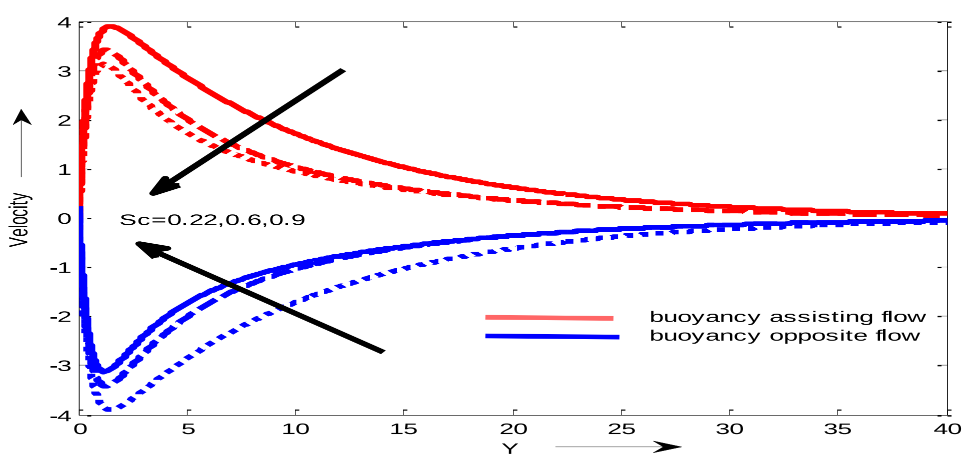

Fig.7.Consequence of *Sc* on Velocity.

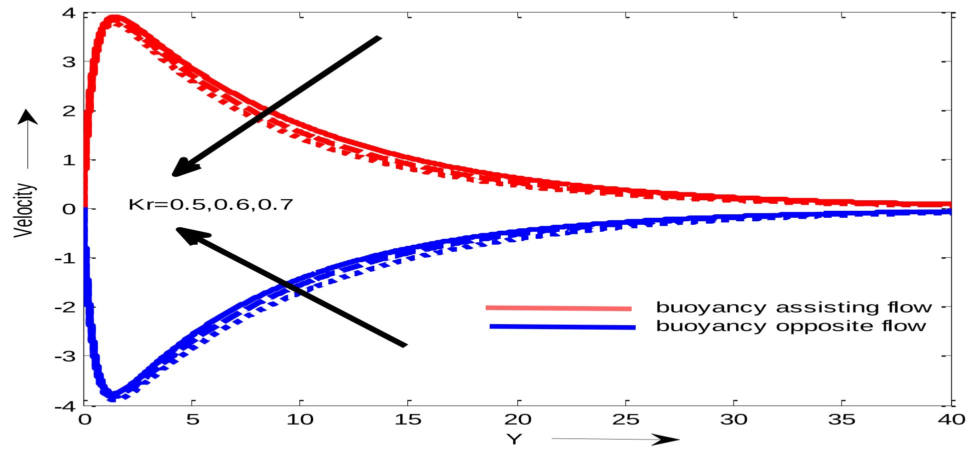

Fig.8.Consequence of *Kr* on Velocity.

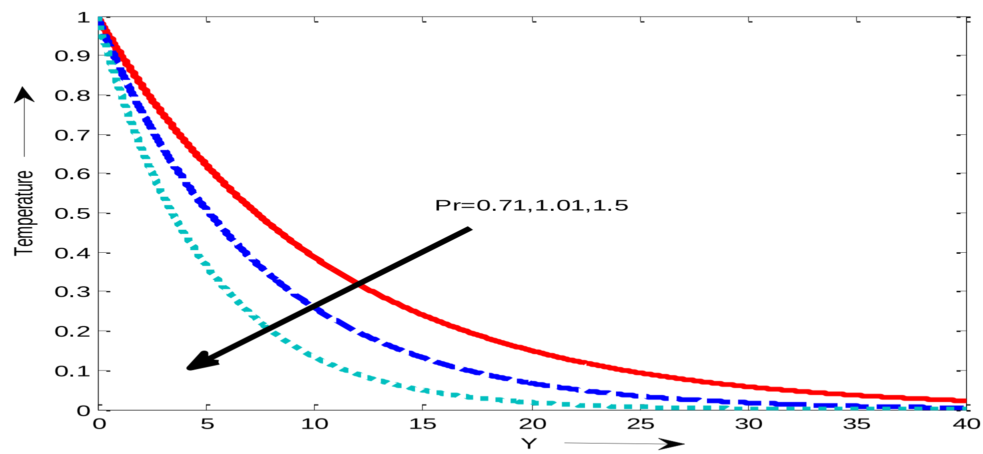

Fig.9.Consequence of *Pr* on Temperature

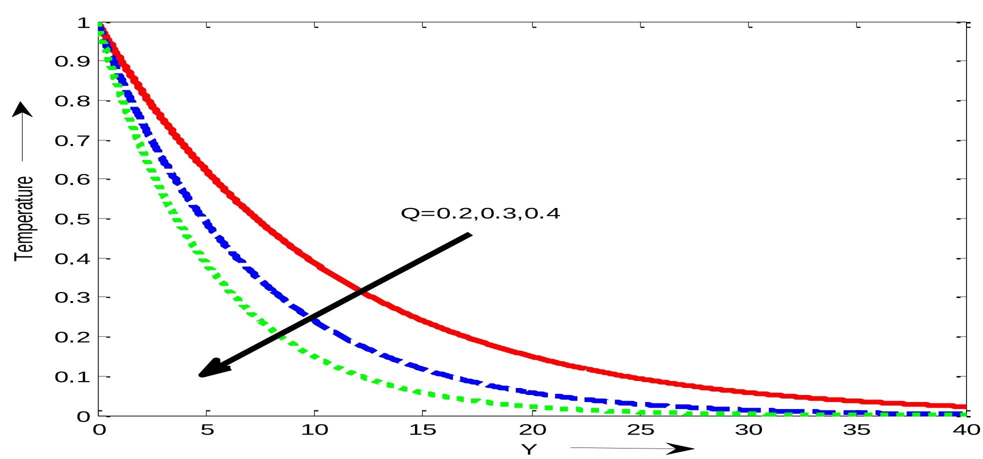

Fig.10.Consequence of *Q* on Temperature

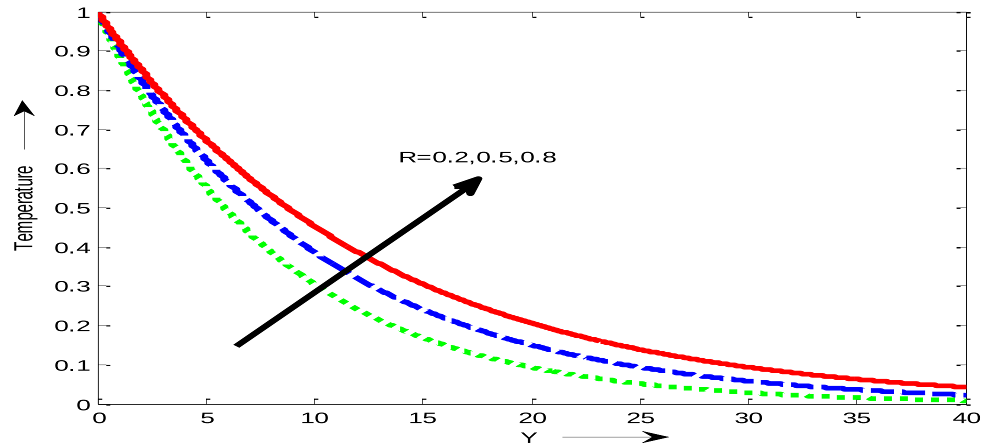

Fig.11.Consequence of *R* on Temperature

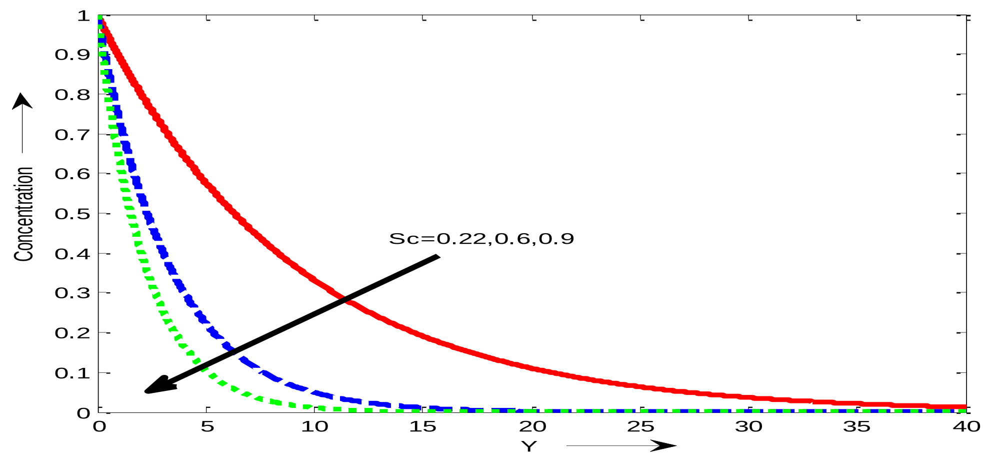

Fig.12.Consequence of *Sc* on Concentration

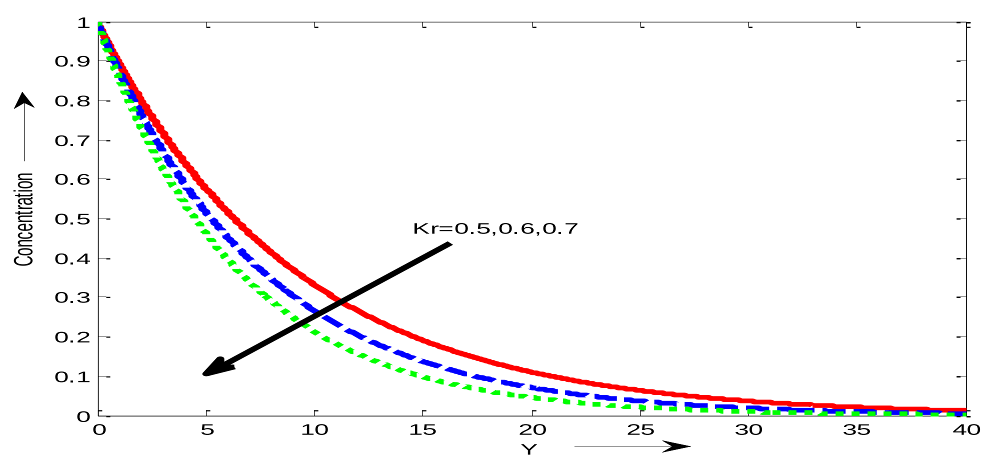

Fig.13.Consequence of *Kr* on Concentration

Table: Skin-friction coefficient, Nusselt number and Sherwood number:

M	λ	Pr	Q	R	Kr	Sc	τ (Gr=5,Gm=5)	τ (Gr=-5,Gm=-5)	Nu	Sh
2	**0.05**	**0.71**	**0.2**	**0.5**	**0.5**	**0.22**	**-9.1054**	**9.1054**	**0.0947**	**0.1100**
3							**-9.2453**	**9.2453**		
4							**-9.3151**	**9.3151**		
	0.15						**-8.3470**	**8.3470**		
	0.2						**-8.0132**	**8.0132**		
		1.01					**-9.0340**	**9.0340**	**0.1347**	
		1.5					**-8.9307**	**8.9307**	**0.2000**	
			0.3				**-9.0216**	**9.0216**	**0.1420**	
			0.4				**-8.9464**	**8.9464**	**0.1893**	
				0.6			**-9.1165**	**9.1165**	**0.0887**	
				0.7			**-9.1264**	**9.1264**	**0.0835**	
					0.6		**-9.1264**	**9.1264**		**0.1320**
					0.7		**-9.0667**	**9.0667**		**0.1540**
						0.6	**-8.8311**	**8.8311**		**0.3000**
						0.9	**-8.7075**	**8.7075**		**0.4500**

CONCLUSIONS:

The findings of the above-mentioned investigation are as follows:

1. It should be observed that while velocity reduces in the buoyancy-opposing zone, velocity increases there with the parameters R, Gm, or Gr With the parameters M, Pr, Q, Kr, or Sc, velocity rises in the buoyancy-helping region while falling in the buoyancy-resistance region.
2. It is known that the temperature field is increased by the radiation parameter while it is decreased by the Pr or Q parameters.
3. A dimensionless concentration field is possible with Kr or Sc.
4. For buoyancy-helping, the skin-friction coefficient rises with growth in, Pr, Q, Sc, or Kr and falls with growth in M or R; the opposite is true for opposing region.
5. The Nusselt number increases when Pr or Q increase, and it only decreases as R increase.

The Sherwood number climbs as Sc or Kr increases.

CONFLICT OF INTEREST

There are no conflicts to declare.

REFERENCES

Angirasa, D., Peterson, G. P., & Pop, I. (1997). Combined heat and mass transfer by natural convection with opposing buoyancy effects in a fluid saturated porous medium. *International Journal of Heat and Mass*

Transfer, *40*(12), 2755-2773.

Pal, D., & Talukdar, B. (2010). Buoyancy and chemical reaction effects on MHD mixed convection heat and mass transfer in a porous medium with thermal radiation and Ohmic heating. *Communications in Nonlinear Science and Numerical Simulation*, *15*(10), 2878-2893.

Makinde, O. D., & Chinyoka, T. (2013). Numerical investigation of buoyancy effects on hydromagnetic unsteady flow through a porous channel with suction/injection. *Journal of Mechanical Science and Technology*, *27*(5), 1557-1568.

Anika, N. N., & Hoque, M. M. (2013). Thermal buoyancy force effects on developed flow considering hall and ion-slip current. *Annals of Pure and Applied Mathematics*, *3*(2), 179-188.

Azad, A. K., Islam, N. M. M., Mithun, C. N., Rifa, T. I., Hasan, M. J., Hossain, R., & Rahman, M. M. (2022). Numerical study on heat and mass transfer characteristics in a confined enclosure with variable buoyancy ratio. *Results in Engineering*, 100569.

Alam et al., 2025. (2025a). *Online Corrective Feedback and Self-Regulated Writing: Exploring Student Perceptions and Challenges in Higher Education*. *15*(06), 139–150. https://doi.org/https://doi.org/10.5430/wjel.v15n6p139

Alam, J., Hossen, M. S., Nawaz, I., Rahman, S., & Mahmood, A. (2025b). *Black Magic and Dark Tourism Impact Mental Well-being of Gender: A Standpoint of Embodiment Theory With Emotional Experience*.

Hossen, M. S., Pauzi, H. B. M., & Salleh, S. F. B. (2023). Enhancing Elderly Well-being Through Age-Friendly Community, Social Engagement and Social Support. *American J Sci Edu Re: AJSER-135*.

Mohd Pauzi, H., & Shahadat Hossen, M. (2025). Comprehensive bibliometric integration of formal social support literature for elderly individuals. *Housing, Care and Support*, 1–17.

Rahman, M. K., Hossain, M. A., Ismail, N. A., Hossen, M. S., & Sultana, M. (2025). Determinants of students' adoption of AI chatbots in higher education: the moderating role of tech readiness. *Interactive Technology and Smart Education*.

Rashed, M., Jamadar, Y., Hossen, M. S., Islam, M. F., Thakur, O. A., & Uddin, M. K. (2025). Sustainability catalysts and green growth: Triangulating evidence from EU countries using panel data, MMQR, and CCEMG. *Green Technologies and Sustainability*, 100305.